Sensitivity Studies of Different Observables to New Physics in Electroweak Quadric Gauge Couplings at Future Lepton Collider Analyses

Anastasia Boushmelev, University of Siegen, Germany

September 9, 2021

Abstract

In this work we will study vector boson scattering processes at high energy e^+e^- colliders and compare Standard Model simulations, using the Standard Model implementation of the Monte Carlo event generator WHIZARD and the QGC UFO model, with new physics models. We will take a look at scalar dimension 8 operators in effective quantum field theories and study their effects on different observables in comparison to the Standard Model. Besides that we will talk about further studies using machine learning frameworks, i.e. MadMiner, for improving studies of new physics models. Here we work in a framework with energy levels of 1.4 TeV and 3 TeV.

Contents

1 Introduction

For studying new physics beyond the standard model (BSM), effective quantum field theories build a successfull framework by introducing effective couplings which describe possible effects induced by new physics. In this work we will focus on the scalar dimension 8 operators S_0 and S_1.
First we simulate the total cross sections of five e^+e^- vector boson scattering processes at 1.4 TeV and 3 TeV using the so called QGC-UFO Model and the Standard Model (SM) implementation in the Monte Carlo event generator WHIZARD to compare those values to the previously simulated results in [1]. After that we extended the UFO model with the dimension 8 operators S_0 and S_1. We create events for all those calculations and plot the transverse momentum, as well as the invariant mass of the vector boson pair to compare all those models.
Finally we repeat those calculations using MadMiner, a Python-based machine learning framework. By the time this report is written, this step has not been done yet but the further steps will be explained in the last chapter of this report.

2 Theory

2.1 Effective Quantum Field Theories

As already mentioned in the introduction effective field theories has multiple advantages when it comes to research of new physics beyond the Standard Model. Some advantages are that e.g. the SM symmetries are respected and S-matrix axioms are satisfied.
The main idea behind effective field theories is that one does power counting and introduces higher dimension operatos which are then supressed by some powers of the high energy mass scale Λ such that the lagrangian becomes

$$\mathcal{L}_{EFT} = \mathcal{L}_{min} + \sum_{i>4} \frac{c_i}{\Lambda_i^n} \mathcal{O}_i, \tag{1}$$

where c_i denotes the referring coupling. One can also define

$$C_i \equiv \frac{c_i}{\Lambda_i^n} \tag{2}$$

which are called *Wilson coefficients*. This Lagrangian comes up from a bottom up approach as using this technique does not require to know the underlying new physics. Next one has to build up the dimension six operator set after writing down $\mathcal{L}_{min}$ using the matrix Higgs representation and then the dimension 8 operators. This has been done in [2] so we will now focus on the scalar dimension 8 operatos which will be relevant in this work.

2.1.1 Dimension 8 Operators

By constructing dimension 8 operators such as in [2], one can find multiple operators which can be categorized into three categories: operators with four field strength tensors (index T), with two derivatives and two Higgs fields (index M) and finally operators which include four derivatives of Higgs fields (index S). Operators with an uneven number of Higgs fields do not contribute to leading order caluclations so we will not dive deeper into this category.
Dimension 8 operators which include four derivatives of Higgs fields represent the scalar operators we will focus on in this work. Those are namely given by

$$\begin{aligned}\mathcal{L}_{S,0} &= F_{S,0}\mathrm{Tr}\left[(\boldsymbol{D}_\mu \boldsymbol{H})^\dagger \boldsymbol{D}_\nu \boldsymbol{H}\right]\mathrm{Tr}\left[(\boldsymbol{D}^\mu \boldsymbol{H})^\dagger \boldsymbol{D}^\nu \boldsymbol{H}\right]\\ \mathcal{L}_{S,1} &= F_{S,0}\mathrm{Tr}\left[(\boldsymbol{D}_\mu \boldsymbol{H})^\dagger \boldsymbol{D}_\mu \boldsymbol{H}\right]\mathrm{Tr}\left[(\boldsymbol{D}^\nu \boldsymbol{H})^\dagger \boldsymbol{D}^\nu \boldsymbol{H}\right].\end{aligned} \tag{3}$$

There is a third scalar dimension 8 operator S_2 but we will ignore this one for that moment as it is isospin violating.

2.2 Vector Boson Scattering

In this work we will study vector boson scattering processes in an e^+e^- collider. Those are

$$e^+e^- \to e^+e^-W^+W^-, \tag{4}$$
$$e^+e^-ZZ, \tag{5}$$
$$\bar{\nu}_e\nu_e W^+W^-, \tag{6}$$
$$\bar{\nu}_e\nu_e ZZ, \tag{7}$$
$$\bar{\nu}_e e^- W^+Z. \tag{8}$$

Turning to the actual measurment simulations at a high energy collider we have to pay attention when choosing cuts in the simulations. The SM simulations are analysed using a center of mass energy of $\sqrt{s} = 1.4$ TeV and $\sqrt{s} = 3$ TeV.
We will especially focus on signals induced by vector-boson pairs with very forward neutrinos and electrons.
We will not pay attention to photon induced W-boson pair production as this vertice does not include new physics effects and leads to divergencies due to the electron photon approximation (EPA). We also ignore detections which dissapear in forward directions in the beampipe such that finally we choose the cuts set up given in table 2.2 from [3].

Parameter	Cut	Supression
$M_{inv}(\bar{\nu}\nu)$	> 175GeV	Background from $Z \to \nu\nu$, W^+W^- and 4 jet prod.
$p_{\perp,W/Z}$ $\lvert\cos\theta(W/Z)\rvert$	> 180GeV < 0.8	Background from t-channel exchange
$p_\perp(WW)$ $p_\perp(ZZ)$ $\theta(e)$	> 50GeV > 40GeV > 15mrad	Background from $\gamma\gamma$ fusion
M_{inv}^{WW} M_{inv}^{ZZ}	$\in [800, 1175]$GeV $\in [800, 1175]$GeV	Massive EW radiation

Table 1: Cuts used in the following vector boson scattering simulations in WHIZARD [3].

3 Computing Framework

3.1 WHIZARD

WHIZARD [4] is a Monte Carlo event generator which can caluclate the total cross sections of multi-particle scattering processes by phasespace integrations. We used the most recent 3.0.1 version for out calculations.
It includes a SM implementation and it can as well understand other models, e.g. the so called QGC-UFO Model. We expect that both models will give similar results to the results from [1].

3.2 MadMiner

MadMiner [5] is a machine learning-based interference for particle physics. Particle physicists are interested in such machine learning mechanisms because of the problem of likelihood-free interference. There are already many tools which calculate hypothetical observations using Monte-Carlo methods, but when it comes to the other way around, those tools are not able to calculate the likelihood function for a set of observables.
There are some approaches for solving this problem, one of those approaches is using machine learning based methods. Those methods often make use of a neural network which train the classification of events and after that a acceptance region is defined.

4 Results

4.1 Results for Cross Sections and other Observables in the Standard Model

In this chapter we will discuss the simulated cross sections for the processes (4) - (8) and compare the results from the calculations using the UFO model, the SM framework given within WHIZARD and the results given in [1]. After that we will implement the cuts given in table 2.2 and again compare those results. But first we will take a look at the SM parameters in the UFO and SM model to check if we can use the UFO model for futher BSM calculations.

4.1.1 Parameters in the SM and the UFO Models

Before doing simulations we have to check whether the results from the UFO model and the SM model are compareable by having the same preliminaries. The model-derived parameters for both models are given in table 4.1.1. We can see that no parameter

Parameter	UFO model	SM model
Derived Parameters		
vev	2.462205690735E+02	2.462205690735E+02
sw	4.714439262191E-01	4.834235829598E-01
cw	8.818960394690E-01	8.753865657173E-01
ee	3.079561542961E-01	3.134506398131E-01
aEW	7.546888109483E-03	$(1.279002939810E+02)^{-1}$

Table 2: Differences between parameters from the UFO and the SM model in WHIZARD.

differs too much between the models and small fluctuations are given by calculation. This means that we can continue with the comparison of cross sections in both models

4.1.2 Without Cuts

First we carry out the SM simulations without cuts. The results are given in table 4.1.2 for a center of mass energy of $\sqrt{s} = 1.4$ TeV and in table 4.1.2 for a center of mass energy of $\sqrt{s} = 3$ TeV.
Independent of $\sqrt{s}$ we can see that the processes $W^+W^-e^+e^-$ and $W^\pm Ze^\pm\nu$ diverge, i.e. integration does not converge. This can also be seen when considering the results from the integrations in each iteration and we can determine that the cross section does not converge against one value. This can be explained by the missing cuts which ensure that e.g. electron photon approximation (EPA) does not cause divergencies along the beam axis. This can be solved by cutting out a certain angle along the beam axis, which

Process	UFO model [fb]	Error [fb]	SM model [fb]	Error [fb]
$W^+W^-\nu\bar{\nu}$	$3.9668936E+01$	$6.11E-02$	$3.8306845E+01$	$6.04E-02$
$W^+W^-e^+e^-$	$2.9432184E+06$	$8.09E+05$	$1.4836900E+03$	$2.27E+01$
$W^\pm Ze^\pm\nu$	$2.6994784E+06$	$1.21E+06$	$1.0807701E+07$	$2.35E+06$
ZZe^+e^-	$4.7051340E+00$	$1.54E-01$	$3.7605598E+00$	$7.25E-02$
$ZZ\nu\bar{\nu}$	$1.5295920E+01$	$2.95E-02$	$1.4068256E+01$	$2.67E-02$

Table 3: Total cross sections with center-of-mass energy $\sqrt{s} = 1.4$ TeV without cuts.

Process	UFO model [fb]	Error [fb]	SM model [fb]	Error [fb]
$W^+W^-\nu\bar{\nu}$	$3.9668936E+01$	$6.11E-02$	$3.8306845E+01$	$6.04E-02$
$W^+W^-e^+e^-$	$2.9432184E+06$	$8.09E+05$	$1.4836900E+03$	$2.27E+01$
$W^\pm Ze^\pm\nu$	$2.6994784E+06$	$1.21E+06$	$1.0807701E+07$	$2.35E+06$
ZZe^+e^-	$4.7051340E+00$	$1.54E-01$	$3.7605598E+00$	$7.25E-02$
$ZZ\nu\bar{\nu}$	$1.5295920E+01$	$2.95E-02$	$1.4068256E+01$	$2.67E-02$

Table 4: Total cross sections with center-of-mass energy $\sqrt{s} = 3$ TeV without cuts.

is also done in the next chapter.
Beside that we can see that the results from both models seem to behave similar and our main goal now is to check, whether the results from the UFO model are compatible with the SM implementation of WHIZARD which seem to be the case.

4.1.3 With Cuts

Now we repeat the simulations with the implementation of the cuts given in table 2.2. The results are given in table 4.1.3 for a center of mass energy of $\sqrt{s} = 1.4$ TeV and in table 4.1.3 for a center of mass energy of $\sqrt{s} = 3$ TeV.

Process	UFO model [fb]	Error [fb]	SM model [fb]	Error [fb]
$W^+W^-\nu\bar{\nu}$	$1.0583859E-01$	$7.71E-04$	$1.0336584E-01$	$7.18E-04$
$W^+W^-e^+e^-$	$1.1182698E+02$	$5.09E+01$	$2.1495165E+01$	$7.13E+00$
$W^\pm Ze^\pm\nu$	$2.1752240E+00$	$1.82E-02$	$2.0032515E+00$	$1.50E-02$
ZZe^+e^-	$1.0585922E-02$	$2.10E-04$	$1.2316917E-02$	$2.43E-04$
$ZZ\nu\bar{\nu}$	$8.2216058E-02$	$5.56E-04$	$7.6601094E-02$	$5.38E-04$

Table 5: Total cross sections with center-of-mass energy $\sqrt{s} = 1.4$ TeV with cuts.

Now we can see that the cuts healed the divergencies and we can start comparing the results from both models. We can directly see that every result (for $\sqrt{s} = 1.4$ TeV as well as for $\sqrt{s} = 3$ TeV) lays within 3σ in both models.

Process	UFO model [fb]	Error [fb]	SM model [fb]	Error [fb]
$W^+W^-\nu\bar{\nu}$	$1.0023240E+00$	$9.22E-03$	$9.6850855E-01$	$1.05E-02$
$W^+W^-e^+e^-$	$1.6991784E+00$	$2.43E-02$	$1.4904859E+00$	$3.28E-02$
$W^\pm Ze^\pm\nu$	$3.8679781E+00$	$3.93E-02$	$3.6001977E+00$	$3.67E-02$
ZZe^+e^-	$4.9496975E-03$	$1.96E-04$	$4.2460384E-03$	$2.33E-04$
$ZZ\nu\bar{\nu}$	$8.5820672E-01$	$1.53E-02$	$7.9395415E-01$	$1.53E-02$

Table 6: Total cross sections with center-of-mass energy $\sqrt{s} = 3$ TeV with cuts.

To visualize the compatibility of both models we use a python script which reads of the .lhe files generated by whizard and plots the transverse momentum distribution and the invariant mass for each process in both models normalized to the total cross section. Those plots are given in 4.1.3 for $\sqrt{s} = 1.4$ TeV and in 4.1.3 for $\sqrt{s} = 3$ TeV.
We can see that with one exception (process (4) at $\sqrt{s} = 1.4$ TeV) all distributions seem to fit in both models. The exception seems to come from statistics or a divergence we have not considered. As this problem is solved with higher energies we are just going to ignore this discrepancy.
All in all we can say that the UFO model and the SM implementation of WHIZARD give compatible results which also fit the results in [1], at least in the orders of magnitude. This is enough as we do not know in which exact environment the simulations were made and how comparable those results are to ours.

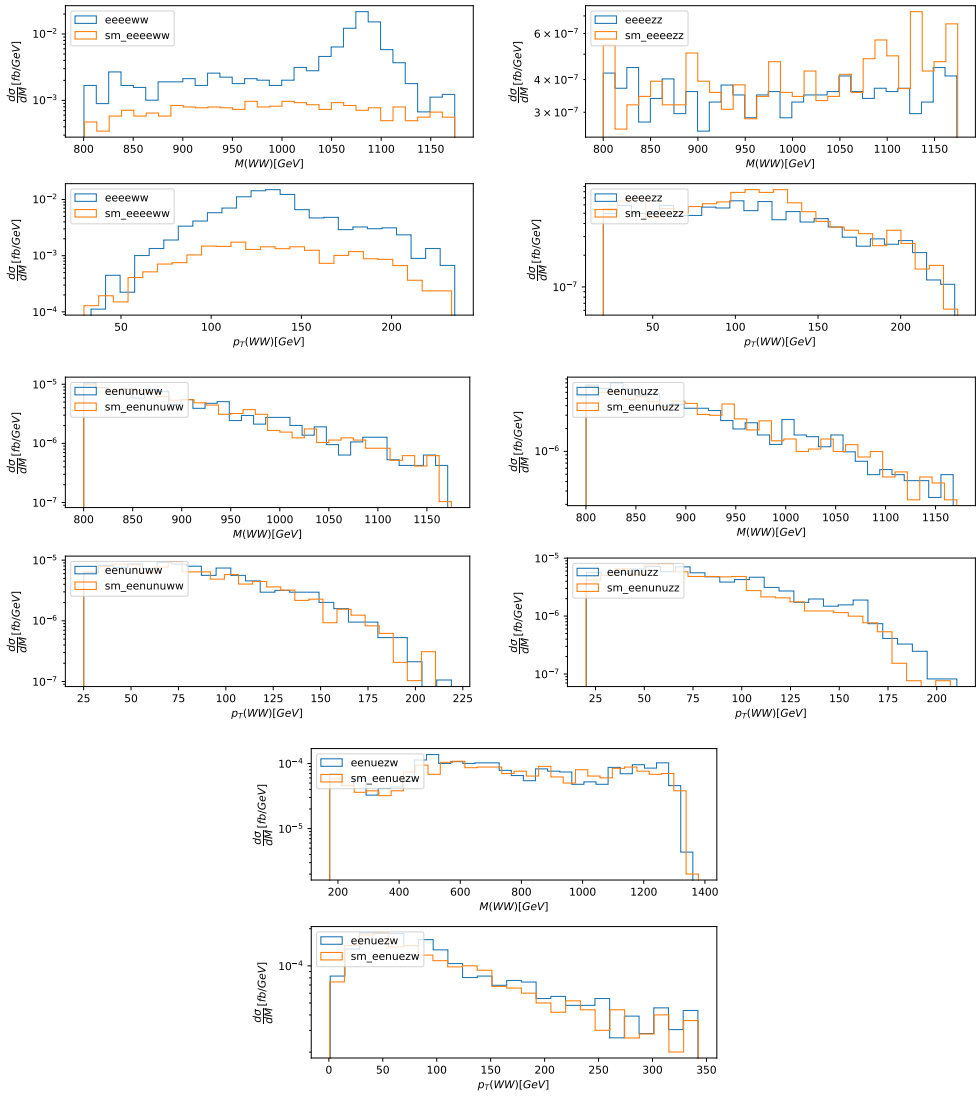

Figure 1: Invarinat mass and transverse momentum distributions of the vector boson pairs for the processe (4)-(8) for a center of mass energy of $\sqrt{s} = 1.4$ TeV.

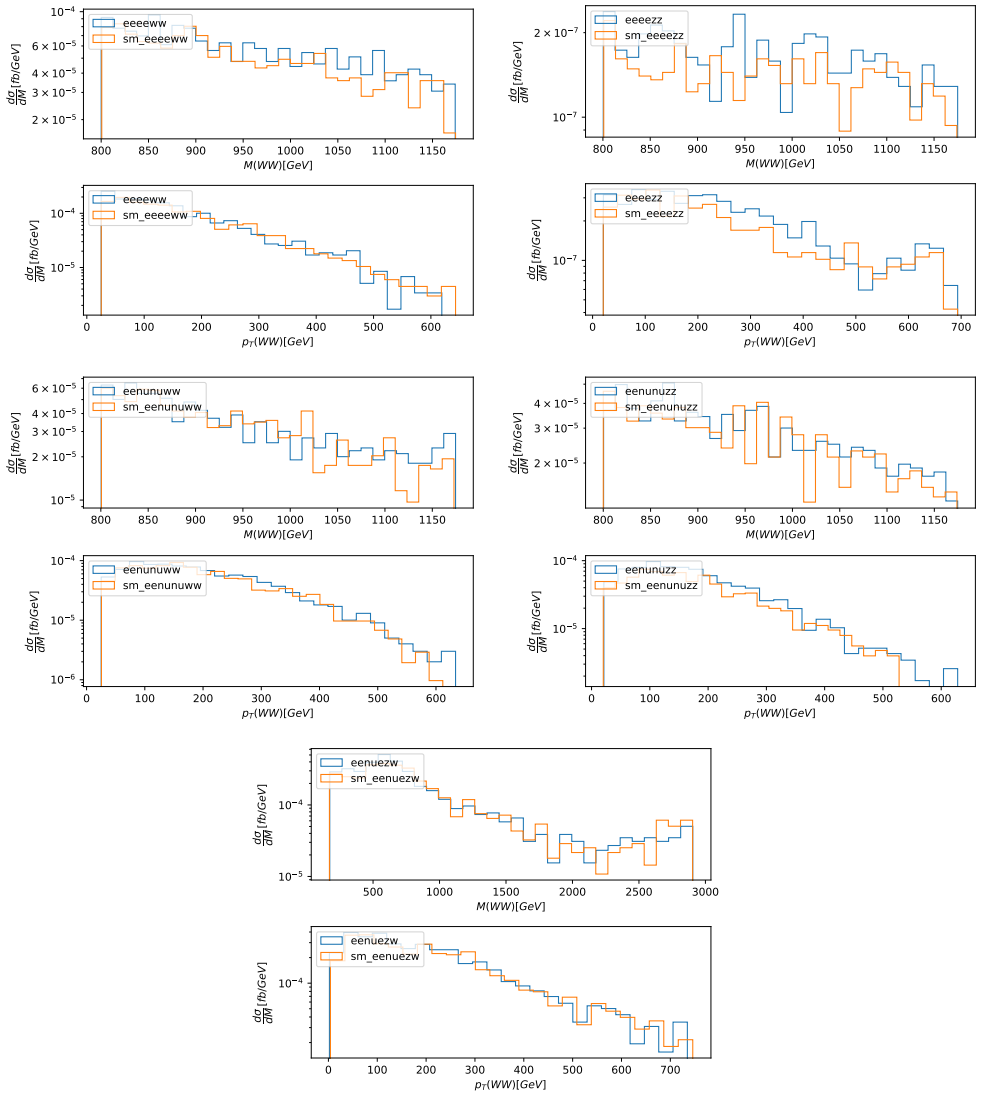

Figure 2: Invarinat mass and transverse momentum distributions of the vector boson pairs for the processe (4)-(8) for a center of mass energy of $\sqrt{s} = 3$ TeV.

4.2 Results for Cross Sections and other Observables Beyond the Standard Model

Next we can move on and unlock the scalar BSM vertices we talked about earlier and simulate cross sections with those in the UFO model. First we will look at the results with the scalar operator S_0 and after that for S_1.

4.2.1 Scalar Operator S_0

The cross sections for all processes are given in table 4.2.2 Now we can compare the mass

Table 7: Total cross sections with center-of-mass energy $\sqrt{s} = 1.4$ TeV with cuts and with the BSM scalar operator S_0.

Process	Cross Section [fb]	Error [fb]
$W^+W^-\nu\bar{\nu}$	$1.0818708E-01$	$7.58E-04$
$W^+W^-e^+e^-$	$2.4353356E+02$	$7.46E+01$
$W^\pm Ze^\pm\nu$	$2.1672855E+00$	$2.59E-02$
ZZe^+e^-	$1.3298471E-02$	$2.91E-04$
$ZZ\nu\bar{\nu}$	$8.2785123E-02$	$6.26E-04$

and transverse momentum distributions of the UFO SM and the BSM results. Those plots are given in figure 4.2.2.

We can see that the biggest differences are given for the processes

$$e^+e^- \to e^+e^-W^+W^- \quad \text{and} \quad e^+e^-ZZ. \tag{9}$$

This can be assigned to the fact, that those effects converege the worst. This can be checked by the accuracy value of the Monte Carlo simulation. Those are shown in table **??**.
Here we can see that all accuarcy values are higher than 2 which is a higher boundary for good convergency. This means that the results for those processes, especially $e^+e^- \to e^+e^-W^+W^-$, are not comparable.
Beside that we can see BSM effects in higher energies.

Table 8: Accuracy of the Monte Carlo simulations in the UFO SM and the BSM model with the scalar operator S_0 respectively S_1

Process	Accuracy
UFO SM	
$W^+W^-e^+e^-$	143.59
ZZe^+e^-	6.26
BSM S_0	
$W^+W^-e^+e^-$	96.71
ZZe^+e^-	6.92
BSM S_1	
$W^+W^-e^+e^-$	95.56
ZZe^+e^-	4.56

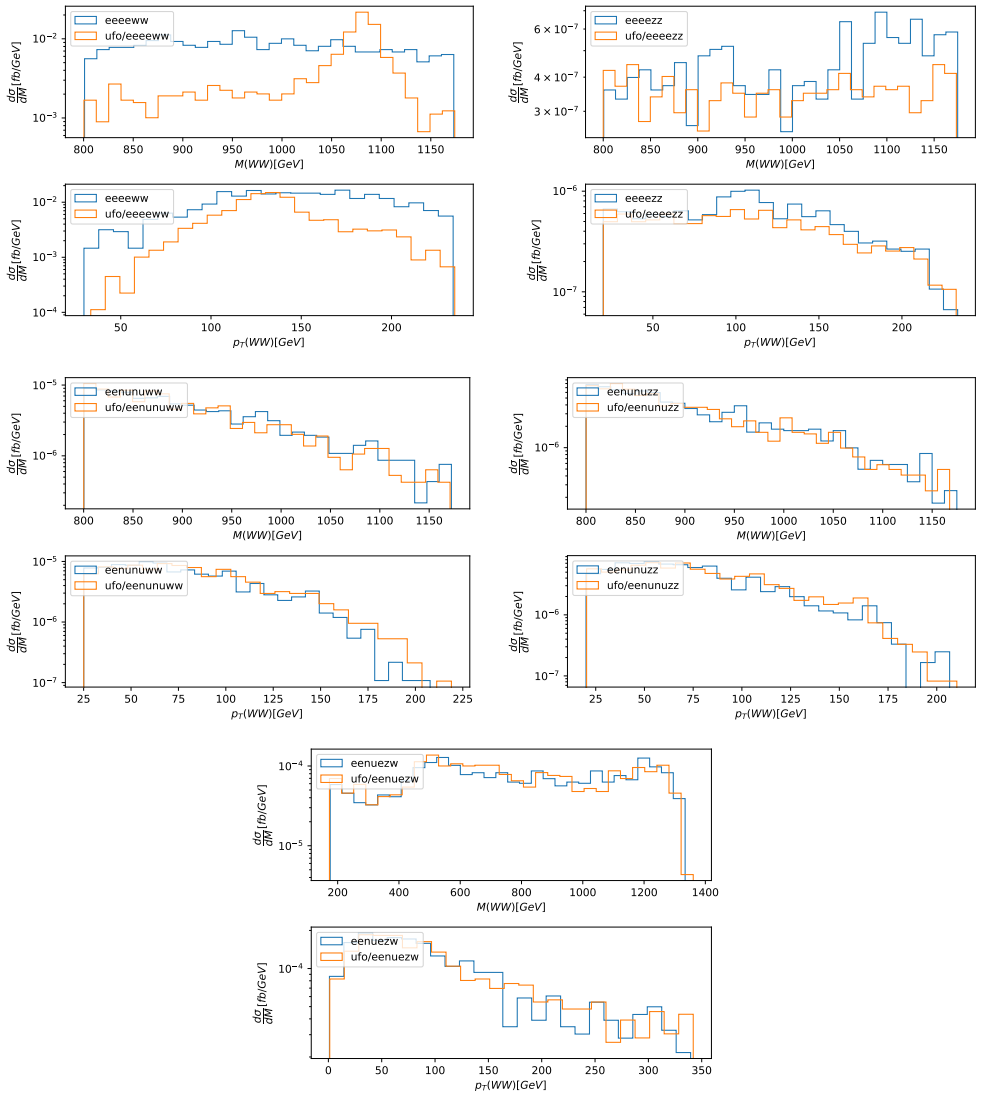

Figure 3: Invariant mass and transverse momentum distributions of the vector boson pairs for the processe (4)-(8) for a center of mass energy of $\sqrt{s} = 1.4$ TeV comparing the SM results (orange) and the BSM results with the unlocked S_0 vertice (blue).

4.2.2 Scalar Operator S_1

The cross sections for all processes are given in table 4.2.2 Again we can compare the

Process	Cross Section [fb]	Error [fb]
$W^+W^-\nu\bar{\nu}$	$1.1264613E-01$	$7.08E-04$
$W^+W^-e^+e^-$	$1.6076141E+02$	$4.86E+01$
$W^\pm Ze^\pm\nu$	$2.1212606E+00$	$1.77E-02$
ZZe^+e^-	$1.3462784E-02$	$1.94E-04$
$ZZ\nu\bar{\nu}$	$8.3966448E-02$	$7.10E-04$

Table 9: Total cross sections with center-of-mass energy $\sqrt{s} = 1.4$ TeV with cuts and with the BSM scalar operator S_1.

mass and transverse momentum distributions of the UFO SM and the BSM results. Those plots are given in figure 4.2.2.
We can see similar results as for S_1.

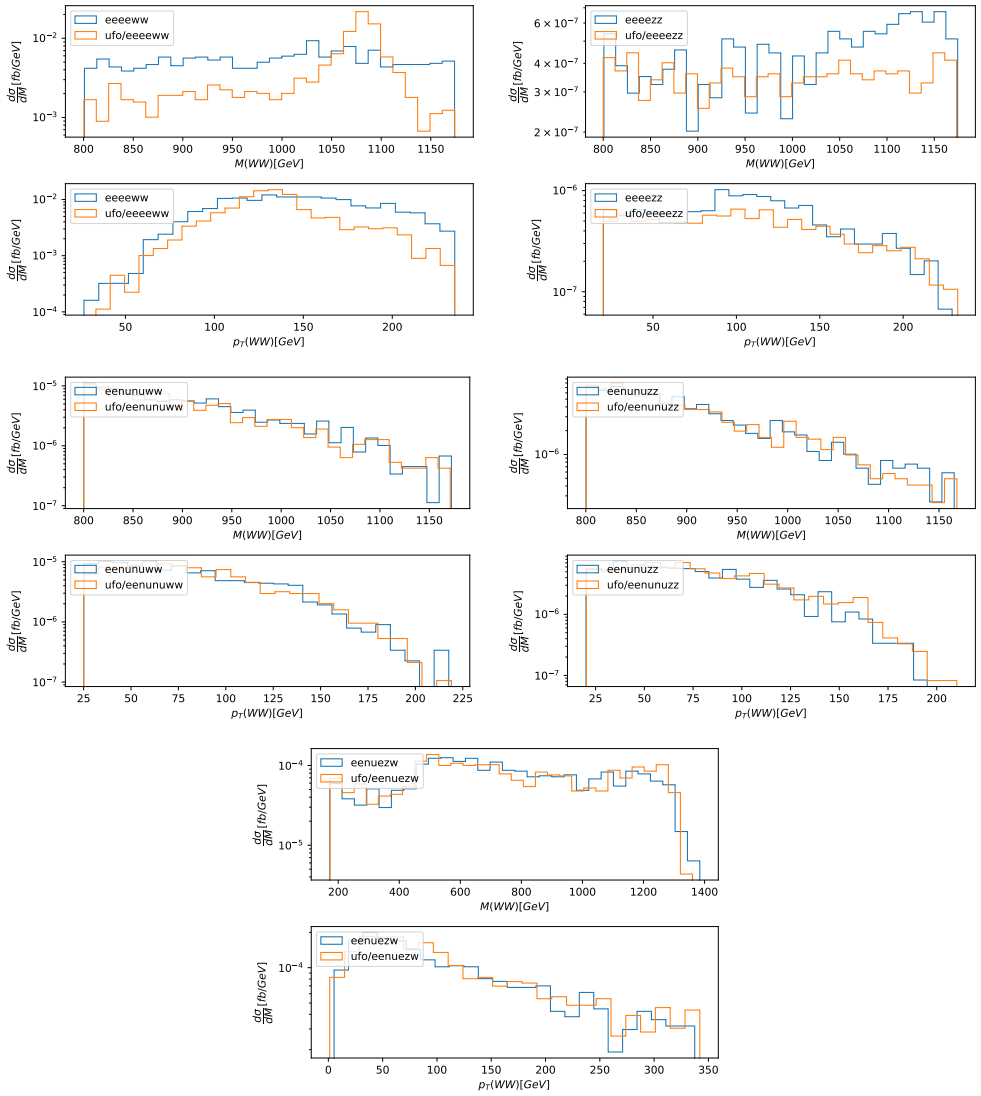

Figure 4: Invariant mass and transverse momentum distributions of the vector boson pairs for the processe (4)-(8) for a center of mass energy of $\sqrt{s} = 1.4$ TeV comparing the SM results(orange) and the BSM results with the unlocked S_1 vertice (blue).

5 Outlook MadMiner

The next step is now to implement the two BSM scalar operators S_0 and S_1 into MadMiner and do the simulations using Machine Learning Tools. For doing that we first have to define the process we will study, including the BSM operators, and do the morphing, which bascially means the interpolation of event weights. This gives us additional benchmark points which we then implement into our WHIZARD simulation and after that we can generate the .lhe file which we then can send through Delphes etc. Finally we can train the model and then do several statistical analysis using MadMiner.
The most difficult part about that proceidure will be, that MadMiner was written to work with .lhe files generated by MadGraph and we have to rewrite the WHIZARD files into a format which MadMiner will understand. We are currently working on that.

6 Conclusion

All in all we can see that using ETF's gives a stable framework for searching for new phyiscs beyond the Standard Model. First we saw that two different Standard Model implementation, namely the QGC UFO model and the SM implementation of WHIZARD, give similar results for the vector boson decays in a e^+e^- collider, such that we can surely use the QGC UFO model for BSM research. Also we learned about the importance of cuts in simulations for cutting of divergencies which made it impossible to compare both models. Anyways one process seemed not to converge perfectly even after implementing those cuts.
After that we included the scalar BSM operators S_0 and S_1 into the UFO SM model and compared the BSM and SM results and saw that we have differences at high energies.

The next steps are the implementation in MadMiner and use machine learning for better results by studying the model. Also we can take a look at vector boson decays in $\mu^+\mu^-$ colliders in the SM model, respectively in EFT.

References

[1] Christian Fleper, Wolfgang Kilian, Jürgen Reuter, and Marco Sekulla. Scattering of w and z bosons at high-energy lepton colliders. *The European Physical Journal C*, 77(2), Feb 2017.

[2] Marco Sekulla. Anomalous couplings, resonances and unitarity in vector boson scattering. 2015.

[3] Juergen R. Reuter. Vector boson scattering at electron colliders. 2021.

[4] The whizard event generator. https://whizard.hepforge.org/. Accessed: 2021-09-01.

[5] Johann Brehmer, Felix Kling, Irina Espejo, and Kyle Cranmer. Madminer: Machine learning-based inference for particle physics, Jan 2020.

[6] P.J. Mohr and D.B. Newell (NIST). Physical constants. 2018.

[7] Tianyi Yang, Sitian Qian, Zhe Guan, Congqiao Li, Fanqiang Meng, Jie Xiao, Meng Lu, and Qiang Li. Longitudinally polarized zz scattering at the muon collider, 2021.

[8] Madminer tutorial. http://theoryandpractice.org/madminer-tutorial/intro.html. Accessed: 2021-09-01.